Observation of slow charge redistribution preceding excited-state proton transfer

D. B. Spry and M. D. Fayer[a)]
Department of Chemistry, Stanford University, Stanford, California 94305, USA

(Received 31 July 2007; accepted 5 October 2007; published online 28 November 2007)

The photoacid 8-hydroxy-*N*,*N*,*N*′,*N*′,*N*′,*N*′-hexamethylpyrene-1,3,6-trisulfonamide (HPTA) and related compounds are used to investigate the steps involved in excited-state deprotonation in polar solvents using pump-probe spectroscopy and time correlated single photon counting fluorescence spectroscopy. The dynamics show a clear two-step process leading to excited-state proton transfer. The first step after electronic excitation is charge redistribution occurring on a tens of picoseconds time scale followed by proton transfer on a nanosecond time scale. The three states observed in the experiments (initial excited state, charge redistributed state, and proton transfer state) are recognized by distinct features in the time dependence of the pump-probe spectrum and fluorescence spectra. In the charge redistributed state, charge density has transferred from the hydroxyl oxygen to the pyrene ring, but the OH sigma bond is still intact. The experiments indicate that the charge redistribution step is controlled by a specific hydrogen bond donation from HPTA to the accepting base molecule. The second step is the full deprotonation of the photoacid. The full deprotonation is clearly marked by the growth of stimulated emission spectral band in the pump-probe spectrum that is identical to the fluorescence spectrum of the anion. © *2007 American Institute of Physics*.
[DOI: 10.1063/1.2803188]

I. INTRODUCTION

Photochemistry is induced by the change in electron distribution that molecules undergo when they are placed in the appropriate electronic excited state. An important class of photochemical reactions is photoinitiated proton transfer using photoacids.[1,2] Proton transfer reactions are among the most widespread and important reactions encountered in chemical and biological processes.[3,4] Under thermal equilibrium conditions proton transfer reactions typically occur on much faster time scales than can be followed by current techniques. Therefore, photoacids have become a valuable approach for studying proton transfer dynamics over the past several decades. As with all photochemistry, generally, the charge redistribution that is a prerequisite for a photochemical proton transfer reaction occurs on an ultrafast time scale, even in liquid solution. Here, we will use photoacidity to demonstrate that the charge redistribution that must occur prior to a photochemical proton transfer reaction can be relatively slow, that is, tens of picoseconds.

A photoacid is a molecule with a pK_a in an electronically excited state that is much lower than in the ground state. Photoacids have been studied for over half a century.[5,6] For certain classes of aromatic molecules, the reduction in pK_a upon excitation can be quite large, often seven units or more. This large increase in acidity can induce either an intramolecular or intermolecular proton transfer reaction. In general, the change in the protonation state of a photoacid results in substantial modifications in its electronic spectrum, which makes it possible to time resolve the deprotonation process. Photoacids' electronic structures and electronic spectra are also sensitive to hydrogen bonding interactions with their surroundings as well as their protonation state. These properties make photoacids an important tool for the study of proton transfer and hydrogen bonding in a wide variety of chemical and biological systems.

Research involving photoacids has been reviewed several times.[1,2,7] Despite the extensive use of photoacids to study proton transfer reactions, the details of the mechanism responsible for excited-state proton transfer (ESPT) is still not fully explicated. Following electronic excitation of a photoacid, it is clear that the charge distribution of the molecule is dramatically altered, which, in turn, reduces the pK_a of the molecule. However, it is unclear whether the electronic state responsible for photoacidic behavior is reached directly by optical absorption or if there is a separate distinct intramolecular charge redistribution process that follows excitation but precedes proton transfer.

It is frequently assumed that the charge redistribution occurs essentially instantaneously upon photoexcitation and that the dynamics observed through spectral changes are due to ESPT. The experiments presented below show that for some systems, charge redistribution preceding proton transfer can take place on time scales as long as tens of picoseconds. The long time scale for charge redistribution occurs because a very specific interaction with the solvent is required. If the possibility of slow charge redistribution is not recognized, spectral changes that are actually associated with charge redistribution may be taken to be part of multistep proton transfer dynamics. In many systems, but not all, charge redistribution can be so fast that it effectively occurs upon optical excitation. However, in systems studied below,

[a)]Electronic mail: fayer@stanford.edu

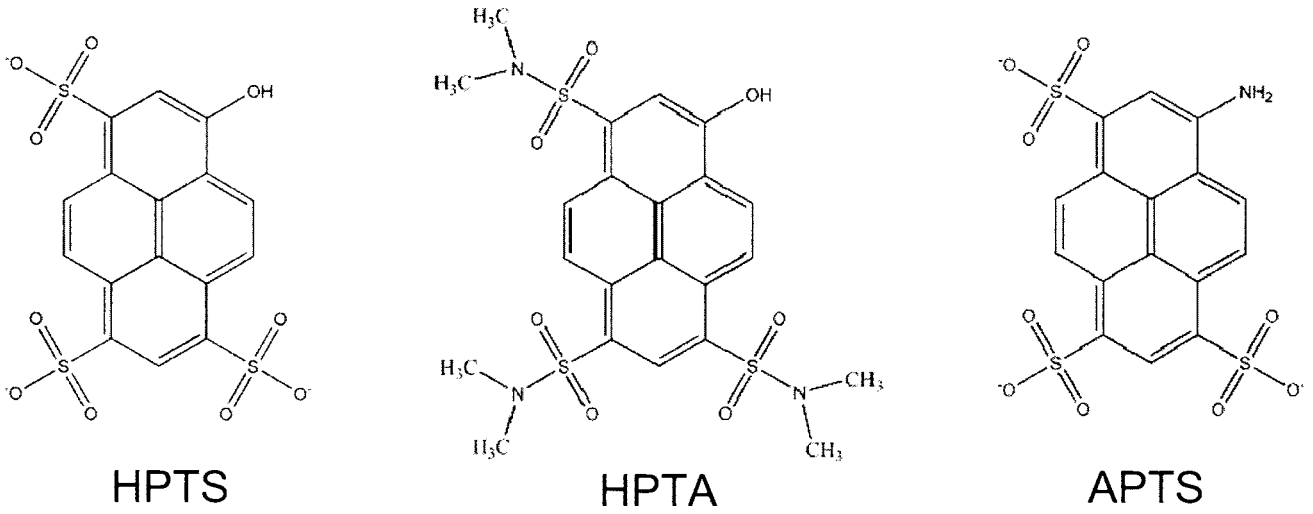

FIG. 1. The structures of the photoacids HPTS and HPTA and the neutral form of APTS.

slow charge redistribution is clearly evident, providing an opportunity to study it and examine its role in excited-state proton transfer.

ESPT has frequently been discussed in terms of an Eigen-Weller model. The Eigen-Weller mechanism for proton transfer is a two-step process.[8,9] Following optical excitation, the initial step is the formation of a contact ion pair, where the acidic proton has transferred from the acid (A) to a base molecule (B), which is frequently a solvent molecule such as water, but the resulting charged species have yet to be separated by the surrounding solvent. The second step is separation of the contact ion pair by the solvent. Solvent separation of the contact pair is followed by additional proton diffusion,

$$AH\cdots B \overset{\text{step 1}}{\rightleftharpoons} [A^-\cdots HB^+] \overset{\text{step 2}}{\rightleftharpoons} A^- + HB^+. \tag{1}$$

The first step is generally taken to be much faster than the second for very strong photoacids and may be limited by the solvent reorganization time.[1,10]

Implicit in Eq. (1) are that the charge redistribution following photoexcitation is so fast that it needs not be considered and that the charge redistribution does not appear in the time dependence of the experimental observables. A more complete description is given in Eq. (2),

$$AH^*\cdots B \overset{\text{step 1}}{\longrightarrow} AH^\dagger\cdots B \overset{\text{step 2}}{\rightleftharpoons} [A^-\cdots HB^+] \overset{\text{step 3}}{\rightleftharpoons} A^- + HB^+. \tag{2}$$

AH^* is the initially excited photoacid. The first step is charge redistribution to form the electronically excited state, $AH^\dagger$. If the charge redistribution is exceedingly fast, it will occur faster than or be mixed in with the solvation and Stokes shift dynamics following the initial excitation, but it will not be manifested on the time scales associated with proton transfer. In such a situation, Eq. (1) will be adequate to describe the dynamics observed experimentally.

In this study, we use a moderately strong pyrene derivative photoacid in several different solvent systems. The photoacid, 8-hydroxy-N,N,N',N',N',N'-hexamethylpyrene-1,3,6-trisulfonamide or HPTA, is a derivative of the well-studied photoacid pyranine, 1-hydroxy-3,6,8-pyrenetrisulfonic acid (HPTS). The structures of these molecules are shown in Fig. 1. The intramolecular charge redistribution step of HPTA is relatively slow and readily observable. In the solvents used here, the excited-state proton transfer is much slower ($\sim$1 ns) than the charge redistribution (tens of picoseconds), which permits clear observation of these two distinct processes. Equation (2) is necessary to understand the HPTA dynamics.

II. EXPERIMENTAL PROCEDURES

HPTS (>98%), HPTA (>95%), and 8-aminopyrene-1,3,6-trisulfonicacid (APTS) (>96%) were purchased from Fluka. dimethyl sulfoxide (DMSO) (anhydrous), dimethyl formamide (anhydrous), and acetonitrile (anhydrous) were purchased from Acros, Inc. Benzene and formamide were purchased from Fisher Scientific. DMSO samples were titrated with a trace amount of dichloroacetic acid to convert HPTA entirely to the protonated state. In all measurements, the chromophore concentrations are $\sim 10^{-4}M$. Because the chromophores used in the experiments are very soluble in all of the solvents, at this low chromophore concentration, there are no interactions between chromophores either in their ground or excited states. Karl-Fischer titrations were performed on a Mettler-Toledo DL32X coulometric Karl-Fischer titrator to determine the amount of water in the samples.

Ultraviolet-visible absorption spectra were measured on a Cary-6000i spectrophotometer. Fluorescence spectra were taken on a Fluorolog-3 fluorescence spectrometer. The spectra were corrected for the Xe lamp intensity profile, monochromator, and photomultiplier response.

Pump-probe experiments in which a particular wavelength is used for the pump and a continuum is used as the probe were performed using a Ti:sapphire regenerative amplified source and a charge-coupled device (CCD) detection system. The pump beam was centered at 400 nm. The excitation used 7 μJ/pulse with 65 fs duration and a spot size diameter of 200 μm. A "white light continuum," used for the probe, was generated by focusing 1–2 μJ of 800 nm light in

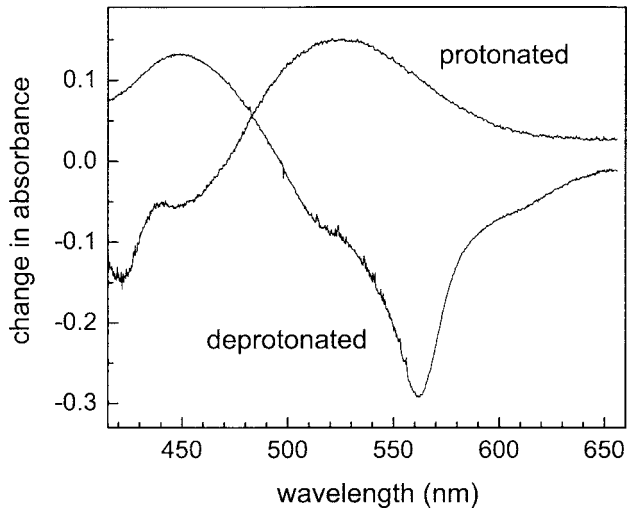

FIG. 2. The pump-probe spectrum of the protonated and deprotonated states of HPTA in acetonitrile at 500 ps.

a 1 mm cuvette of water. A half-wave plate/polarizer combination was used to attenuate the 800 nm light to give the most stable white light. The continuum generated ranged from the near-IR to somewhat beyond 390 nm. The white light was separated into two beams with a beam splitter. One beam was used as the probe and crossed with the pump in the sample, and the other one was used as a reference to monitor the intensity and spectral characteristics of the white light. The timing between the pump and the probe was achieved by passing the pump beam down a high-resolution delay line with ~1 fs resolution. The probe and reference beams were focused into two optical fibers. The outputs of the fibers are at the entrance slit of a 0.3 m monochromator. The dispersed outputs of the two input beams are detected by a 1340×100 pixel CCD detector. The probe and reference produce separately readout stripes on the CCD, which are used to obtain the difference absorption spectrum between pump on and pump off. The reference spectrum permits correction for variation over time of the white light characteristics.

A Ti:sapphire oscillator was used as the excitation source in the time correlated single photon counting (TCSPC) experiments. The laser wavelength was set to 790 nm and the output beam was focused into an acousto-optic pulse selector, which produced pulses at 4 MHz. The single pulses were frequency doubled and used for excitation. Excitation polarization was controlled by a half-wave plate placed immediately before the sample and was set to the magic angle. The emitted photons were collected in front-face geometry and passed through a fixed-angle polarizer before entering a monochromator. The photons were detected with a Hamamatsu microchannel plate detector. The instrument response function was ~45 ps full width at half maximum. All measurements were carried out at room temperature.

III. RESULTS AND DISCUSSION

A. Two-step ESPT process

The pump-probe spectra without excited-state proton transfer of both the protonated and deprotonated states of

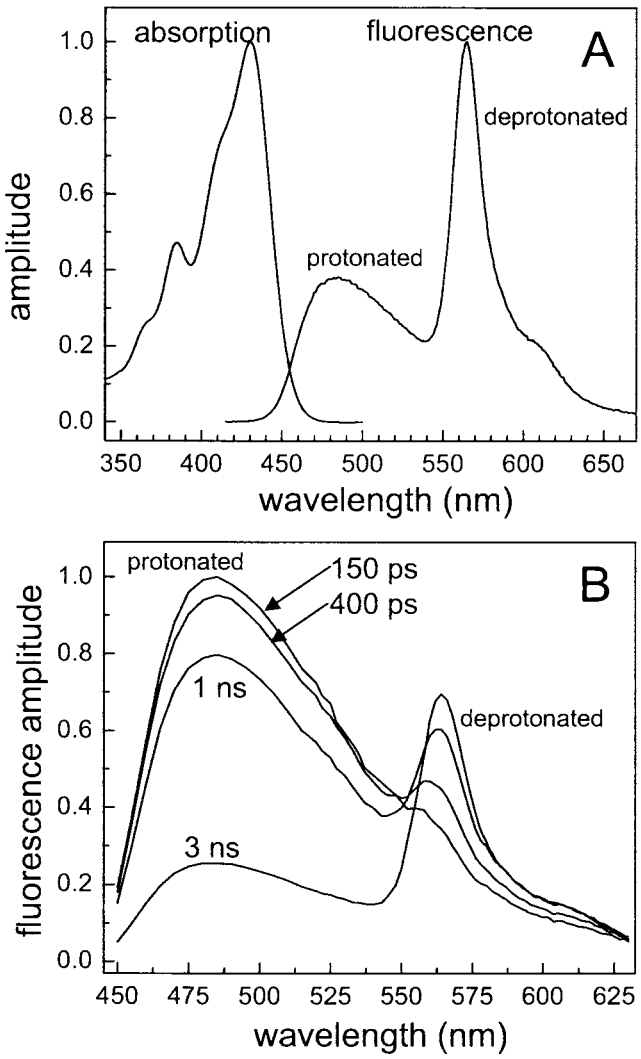

FIG. 3. (A) The steady-state absorption and fluorescence spectra of HPTA in DMSO. (B) The TCSPC fluorescence spectra of HPTA in DMSO at 150 ps, 400 ps, 1 ns, and 3 ns.

HPTA in acetonitrile are shown in Fig. 2. HPTA cannot undergo excited-state proton transfer in acetonitrile. By 500 ps, the time at which the spectra were recorded, all possible solvation processes are complete. The deprotonated form was obtained by adding the base triethylamine. The pump-probe spectra of HPTA show the same bands that are reported for HPTS.[11,12] The protonated state has an excited-state absorption maximum at 525 nm and a stimulated emission maximum at ~445 nm. The negative peak at ~420 nm corresponds to a ground-state bleach, which agrees with the absorption spectrum. The deprotonated state shows an excited-state absorption peak at 450 nm and stimulated emission peak at 560 nm. The deprotonated ground-state bleach appears as a negative shoulder at around 500 nm.

Figure 3(a) shows the steady-state absorption and fluorescence spectra of HPTA in DMSO. Absorption spectra for both the protonated and deprotonated forms of HPTA are found in the Appendix. The absorption spectrum confirms that the HPTA exists exclusively in the protonated state before photoexcitation. The steady-state fluorescence spectrum

demonstrates that a significant amount, but not all, of the ESPT occurs within the excited-state lifetime. This is an initial indication that the ESPT is relatively slow. The time-resolved fluorescence spectra collected by TCSPC are displayed in Fig. 3(b) [note the different frequency axis from Fig. 3(a)]. Under 100 ps, HPTA is almost entirely in the protonated state. As time increases to a few nanoseconds, the sharp fluorescence peak from the deprotonated HPTA anion state centered at ~560 nm grows in approximately as a single exponential with a time constant of ~700 ps. The proton transfer occurs on a time scale that is slow compared to diffusive solvent separation of the contact pair. Therefore, a negligible concentration of the contact pair builds up, and the presence of the contact pair is not observable in the spectroscopic data. Rather, the data display the formation of the charge transfer species, $AH^{\dagger}$, followed by the appearance of the solvent separated photoacid anion and the solvated proton, $A^{-}+HB^{+}$ [see Eq. (2)].

To determine if there is an influence of water in the DMSO on the observed kinetics, the water content of the samples were analyzed using the Karl-Fischer titration. The measured water concentration in the samples was 300 ppm. At this water concentration, the average separation between water molecules is 46 nm. The concentration of water molecules is significantly greater than the concentration of HPTA. Therefore, the time for a water molecule to encounter an HPTA molecule is approximately the time for water to sample the entire liquid volume. The diffusion constant of a water molecule in DMSO was calculated with the Stokes-Einstein equation to be 0.5 nm^2/ns. In the characteristic time observed for proton transfer (~1 ns), the rms diffusion distance of water is 1.7 nm. Because this is only a very small fraction of the average separation between water molecules, the majority of the solvent is not sampled by water on the time scale of interest. The rms displacement is proportional to $t^{1/2}$. A water molecule still will have only sampled 5.4 nm in 10 ns. Therefore, the kinetics are not influenced by the very small amount of water in the samples. To confirm that the water plays no role in the measurements, the experiments were also performed following the addition of water to a sample. The water content was increased ten times to 3000 ppm. The addition of this amount of water did not change the results.

The short time pump-probe spectra of HPTA in DMSO are shown in Fig. 4(a). At 100 fs, the pump-probe spectrum is essentially the same as the protonated state displayed in Fig. 2. The transient absorption spectrum undergoes substantial transformation at relatively short times (tens of picoseconds) compared to the 700 ps time constant for anion production [Fig. 3(b)]. The initial excited-state absorption at ~550 nm changes to stimulated emission as time progresses, and the short time stimulated emission at ~450 nm becomes the excited-state absorption. There is also a very sharp isosbestic point near 500 nm. The isosbestic point indicates a distinct chemical process with two states, and because it is so well-defined in the first few picoseconds, the solvation response (Stokes shift) of HPTA is apparently small.

At times greater than ~70 ps, a pronounced negative, going relatively narrow stimulated emission peak appears at

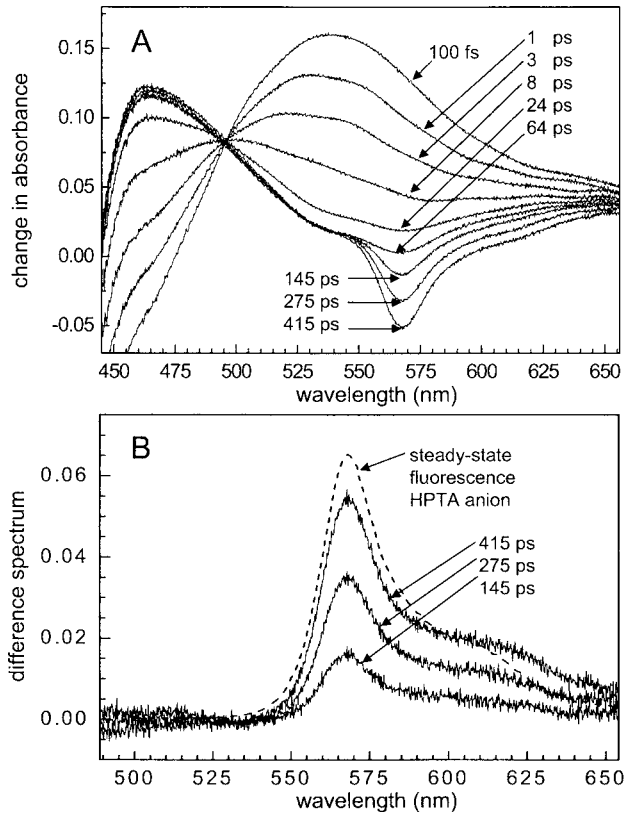

FIG. 4. (A) The pump-probe spectra of HPTA in DMSO at 100 fs, 1 ps, 3 ps, 8 ps, 24 ps, 64 ps, 145 ps, 275 ps, and 415 ps. (B) The difference between the pump-probe spectra shown in Fig. 9(a) at 64 ps and the spectra at 145, 275, and 415 ps. All of the changes to the pump-probe spectrum after 64 ps are caused by the appearance of stimulated emission from the anion of HPTA. The fluorescence spectrum of the HPTA anion in DMSO is included for comparison (dotted line).

~565 nm. This peak corresponds to the fluorescence spectra of the HPTA anion, as can be seen in Figs. 3(a) and 3(b). At longer times, there is no change in the excited-state absorption band from 400 to 550 nm in the pump-probe spectrum, within experimental error. Figure 4(b) displays different spectra taken by subtracting the pump-probe spectrum at 64 ps from spectra taken at later times [note the different frequency axis from Fig. 4(a)]. Also shown is the steady-state fluorescence spectrum of the HPTA anion (dashed line). The difference spectra show clearly that the longer time scale dynamics, greater than ~100 ps, are caused by the growth of stimulated emission from the HPTA anion, that is, the deprotonated state. The difference spectra agree quite well with the steady-state HPTA anion fluorescence spectrum. The data presented in Figs. 4(a) and 4(b) demonstrate that the dynamics following the optical excitation are divided into two time ranges. There are shorter time dynamics (tens of picoseconds) in which there is no evidence of anion production, followed by the anion formation with a ~700 ps time constant.

The short-time dynamics occurring under ~70 ps can be described almost perfectly by a two-component model. Figure 5(a) shows that all of the transient absorption spectra of HPTA in DMSO (data in black) from 400 fs to 64 ps can be described by a linear combination of two spectral components (model calculations in red),

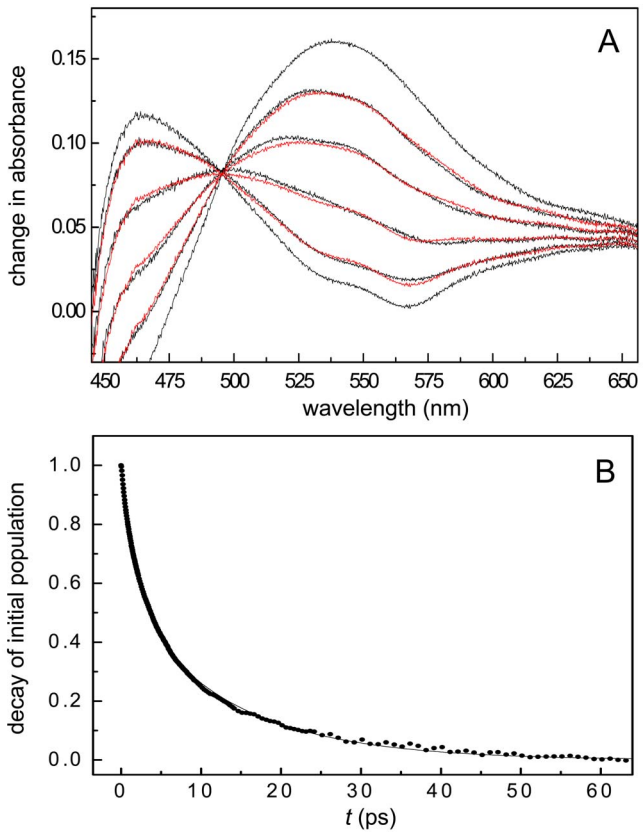

FIG. 5. (Color online) (A) The two-component model (red) applied to data (black) shown in Fig. 9(a) under 64 ps. Pump-probe spectra at 400 fs and 64 ps were used as the basis sets in the model. Computed times: 1, 3, 8, and 24 ps. (B) The weighting coefficient $\alpha(t)$ in fitting the two-component model (dots) fit to a biexponential decay. Time scales for decay are 2.3 ps (46%) and 13.4 ps (54%).

$$f(\omega,t) = \alpha(t)\nu_1(\omega) + (1 - \alpha(t))\nu_2(\omega). \tag{3}$$

Here, $\nu_1(\omega)$ is the spectrum of the initial component, which is the protonated state (chosen at 400 fs to remove the very fast solvation response) and $\nu_2(\omega)$ is the spectrum at 64 ps, which is essentially the spectrum of the state formed prior to proton transfer. 64 ps was chosen to avoid substantial contamination from the anion spectrum. Therefore, the 64 ps spectrum may have a small contribution from the initial protonated state as well as a small contribution from the deprotonated state. A single parameter, $\alpha(t)$, describes the relative weighting of the initial protonated state and the intermediate state that is formed prior to deprotonation. It will be discussed below that this intermediate state is produced by charge redistribution that occurs prior to proton transfer. As can be seen in Fig. 5(a), the superpositions of the spectral components (red) reproduce the measured spectra (black) quite well. A plot of $\alpha(t)$ (points) is given in Fig. 5(b). $\alpha(t)$ fits well to a biexponential decay (solid curve) with time constants (and relative weighting) of 2.3 ps (0.46) and 13.4 ps (0.54). The reported long time component of the solvation of coumarin in DMSO is 2 ps.[13] Approximately half of the dynamics occurs on the time scale of solvation in DMSO.

As shown in Fig. 6(a), the same type of spectral response of HPTA in DMSO demonstrated in Fig. 4(a) continues to

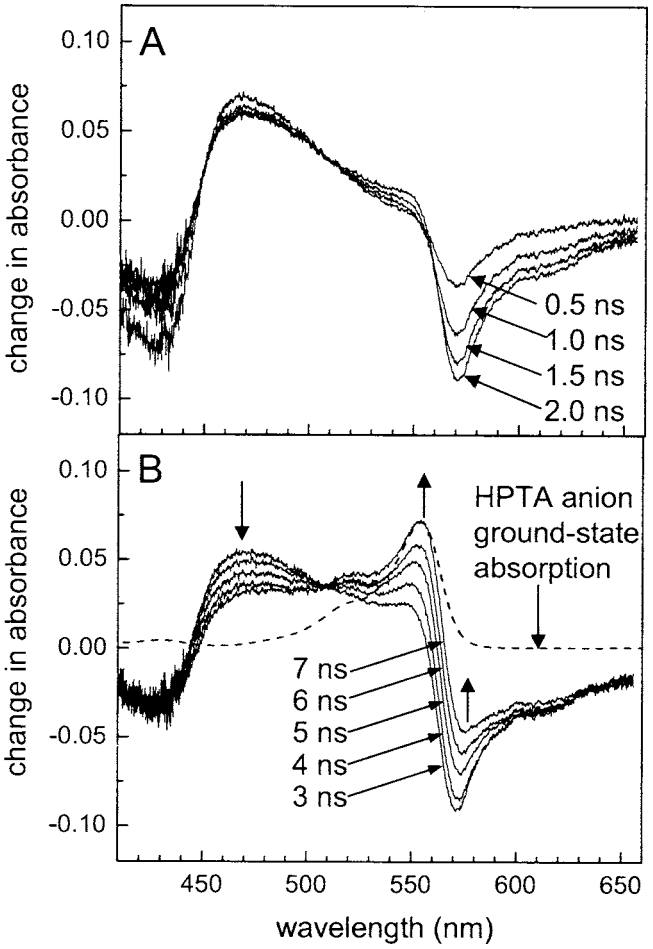

FIG. 6. (A) Pump-probe spectra of HPTA in DMSO at 0.5, 1, 1.5, and 2 ns. Increased stimulated emission at 570 nm is from the increase in the HPTA anion concentration. The increase demonstrates occurrence of ESPT. (B) Longer time pump-probe spectra at 3, 4, 5, 6, and 7 ns. Lifetime decay of the deprotonated excited state (seen at 460 and 570 nm) is coupled with appearance of the ground-state absorption spectrum of the anion (dashed line).

even longer times. For times shorter compared to the excited-state lifetime of the HPTA anion (5.4 ns), the deprotonated state (anion) stimulated emission steadily increases in the pump-probe spectrum. The rate of growth of stimulated emission is consistent with the growth of deprotonated fluorescence measured by TCSPC [Fig. 3(b)]. The rest of the pump-probe spectrum is relatively constant with exception of the ground-state bleach, which fills in due to the short lifetime of the protonated state (1.7 ns). Figure 6(b) shows the dynamics at still longer times where the lifetime decay of the deprotonated state is visible. As the deprotonated state decays to the ground state, the ground-state absorption spectrum of the HPTA anion (dashed line) grows into the pump-probe spectrum.

B. The charge redistribution step

The data presented above are explained in terms of a two-step mechanism that follows optical excitation [see Eq. (2)]. Step 1 is a relatively slow charge redistribution process, and step 2 is even a slower proton transfer. The progression of events is shown clearly by the data in Fig. 4(a). The spec-

trum of HPTA evolves on a time scale of hundreds of femtoseconds to many picoseconds and then, the stimulated emission spectrum of the HPTA anion grows in on the hundreds of picoseconds to nanosecond time scales. Additional experiments discussed below demonstrate that the intermediate state is indeed a charge redistribution state.

Intramolecular charge transfer reactions have been extensively investigated in the past two decades.[14–16] Most of the widely used compounds, for example, *N*,*N*-dimethylaminobenzonitrile,[15] betaine-30,[17] or arylaminonaphthalene sulfonates,[18] have structures that are quite similar to photoacids. These charge transfer chromophores consist of an aromatic ring with both electron donating and electron withdrawing functional groups that work in a "push-pull" fashion to transfer electron density from the electron donor to the ring. These intramolecular electron transfer processes are adiabatic and typically occur on fast time scales that can be much faster than or on the order of the solvent molecular reorientation time.[16,18]

APTS (structure given in Fig. 1) was used here to observe relatively slow intramolecular charge redistribution in the absence of proton transfer. APTS is closely related to HPTA and HPTS. APTS in its neutral form cannot undergo ESPT. (It is a very strong photoacid when the amine is protonated to give NH_3^+.) The structure of APTS is analogous to many of the chromophores used to observe intramolecular electron transfer dynamics. The electronic structure is quite similar to HPTS, except that the amine group of APTS is a much stronger π donor than hydroxyl group of HPTS.

The electron withdrawing strength of the sulfonate functional groups is increased by accepting hydrogen bonds from the solvent.[19] The donation of a hydrogen bond from the solvent to the sulfonate groups stabilizes the negative charge, which leads to a greater pull of electron density from the pyrene ring. This effect can be seen by comparing the excited-state dynamics of APTS in dimethylformamide (DMF) to formamide. Figure 7(a) shows time dependent pump-probe data for APTS in DMF, which is an aprotic solvent that cannot donate hydrogen bonds. In the aprotic solvent, the time dependence of the pump-probe spectrum is produced only by a Stokes shift. The major band at ~525 nm is excited-state–excited-state absorption that shifts to the blue with time, but the shape is essentially unaltered. The maximum shift occurs in ~12 ps. The time dependent frequency correlation function,[20] which is a measure of the time dependence of the Stokes shift, decays with a 3 ps time constant, This time constant is in reasonable agreement with time-resolved studies of coumarin in DMF.[13] Data at 400 ps, which are the same as the data at 12 ps, are shown to demonstrate that there is no further evolution in the spectrum following the Stokes shift.

Formamide is structurally very similar to DMF, but it is a strong hydrogen bond donor. Formamide increases the electron withdrawing ability of the sulfonate groups, making intramolecular charge redistribution (electron transfer) favorable. Figure 7(b) shows time dependent pump-probe data for APTS in formamide. The data are dramatically different from those shown in Fig. 7(a). As time progresses excited-state absorption at wavelengths longer than 500 nm turns into a stimulated emission, and an excited-state absorption peak grows at 475 nm. For APTS in formamide, the dynamics seem very similar to those observed for HPTA [Fig. 6(b)] at short to moderate times, prior to the appearance of the anion stimulated emission produced by proton transfer. There is also an isosbestic point at 500 nm for APTS in formamide, which is in agreement with the pump-probe spectra of HPTA shown in Fig. 4(a). The sharp excited-state absorption peak at ~480 nm grows with a 5.4 ps time constant and matches the solvation dynamics of HPTS in formamide.[12]

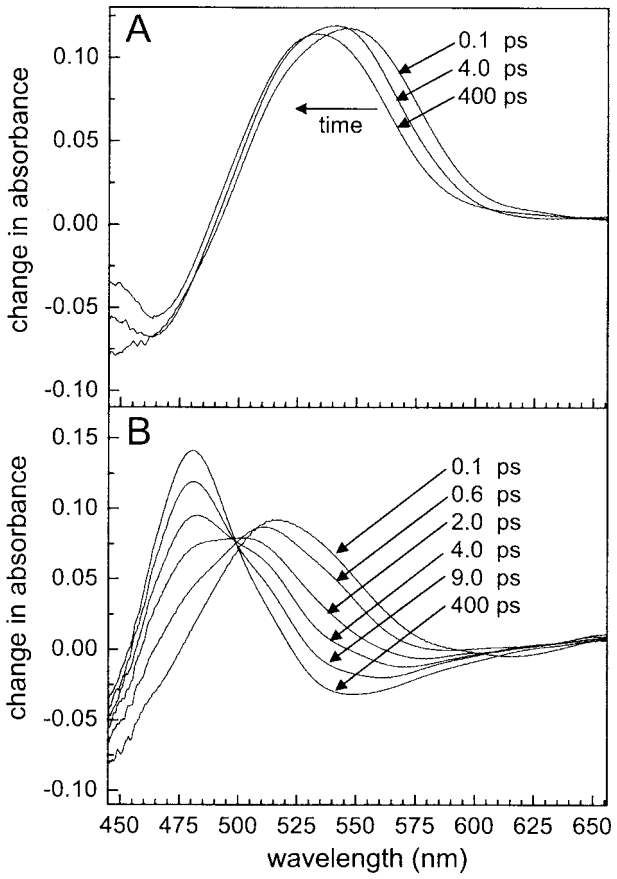

FIG. 7. (A) Pump-probe spectra of APTS in DMF displaying a time dependent Stokes shift at 100 fs, 4 ps, and 400 ps. (B) Pump-probe spectra of APTS in formamide at 100 fs, 600 fs, 2 ps, 4 ps, 9 ps, and 400 ps showing the intramolecular charge transfer process. APTS cannot undergo proton transfer. The 400 ps trace shows the long term limit, which is reached in ~25 ps.

APTS, which cannot undergo proton transfer, displays dynamics in formamide [Fig. 7(b)] that are essentially the same as the short time dynamics of HPTA [Fig. 4(a)] prior to proton transfer. In DMF, the dynamics of APTS only show a time dependent Stokes shift with little other changes in the spectrum. However, in the hydrogen bond donating solvent formamide, APTS can undergo charge redistribution because the sulfonate functional groups act as better electron withdrawing substituents and intramolecular charge transfer is favorable. Because of the similarity in the time dependent spectral data of APTS [Fig. 7(b)] and the time dependent spectral data of HPTA [Fig. 4(a)] at short times $< \sim 100$ ps, we assign the short time dynamics of HPTA to charge redistribution. As shown in Figs. 3 and 4, the short time HPTA

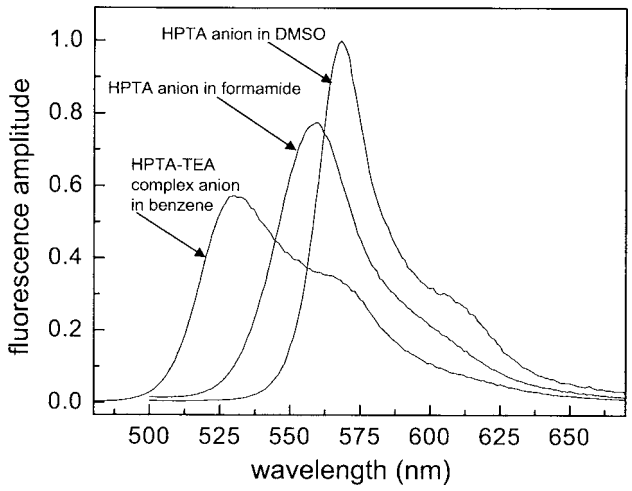

FIG. 8. The fluorescence spectra of the HPTA anion in different hydrogen bonding environments. Shown are HPTA anions in DMSO, formamide, and the HPTA-triethylamine complex in benzene. The HPTA anion fluorescence is normalized for constant oscillator strength.

charge redistribution is followed on the hundreds of picoseconds to nanosecond time scale by proton transfer.

C. Charge distribution and hydroxyl oxygen hydrogen bonding

There is substantial evidence that, in general, the strength of a hydrogen bond donated from a photoacid to an accepting base molecule increases upon photoexcitation.[10,21,22] The increase in hydrogen bond donation has been shown to be particularly significant for HPTA.[23] Figure 8 shows HPTA anion fluorescence spectra in three dramatically different hydrogen bond donating environments. In DMSO and formamide, NaOH base was added to the solutions to assure that the steady-state fluorescence comes exclusively from the HPTA anion. The spectrum labeled as "HPTA-TEA complex anion in benzene" is a different situation. HPTA will not photodissociate in benzene. Rather $10^{-3}M$ triethylamine (TEA) was added to the $10^{-4}M$ HPTA solution. HPTA and TEA form a strong hydrogen bonded complex in the ground state. With a $10^{-4}M$ HPTA concentration and a $10^{-3}M$ TEA concentration in benzene solution, there is no uncomplexed HPTA. As discussed in detail below, the HPTA-TEA complex undergoes extremely fast proton transfer. Therefore, all steady-state fluorescence occurs from the anion.

The spectra in Fig. 8 demonstrate the large influence that the hydrogen bond donation to the deprotonated hydroxyl group of the HPTA anion has on the charge distribution of the π system in the first excited state. The change in charge distribution is manifested by the differences in the fluorescence spectra. The fluorescence spectrum in DMSO is furthest to the red (peak maximum at 568 nm). DMSO is an aprotic solvent that cannot donate a hydrogen bond to the deprotonated hydroxyl functional group of HPTA. The spectrum in formamide is somewhat blueshifted (peak maximum at 560 nm). Formamide has a polarity similar to DMSO and has similar hydrogen bond accepting characteristics. However, formamide can donate a hydrogen bond to the HPTA anion hydroxyl oxygen. HPTA-formamide spectrum is not only blueshifted relative to the DMSO spectrum but it is also significantly broadened. The shift and broadening arise from HPTA accepting a hydrogen bond from formamide. The largest blueshift and greatest broadening occur for the HPTA-TEA complex in benzene. As shown in connection with Fig. 9, essentially all of the steady-state fluorescence comes from the anion because of very rapid proton transfer upon excitation. Benzene has a very low dielectric constant of 2.3, which prevents the separation of the contact ion pair formed in the proton transfer reaction. The result is a very strong hydrogen bond between the triethylammonium cation and deprotonated HPTA anion in the excited state. The specific hydrogen bonding interaction between the ion pairs significantly broadens and blueshifts the fluorescence spectrum of the HPTA anion. The spectra in Fig. 8 show the substantial influence a hydrogen bond interaction with the hydroxyl oxygen has on the excited-state anion spectrum and, therefore, on the electronic charge distribution.

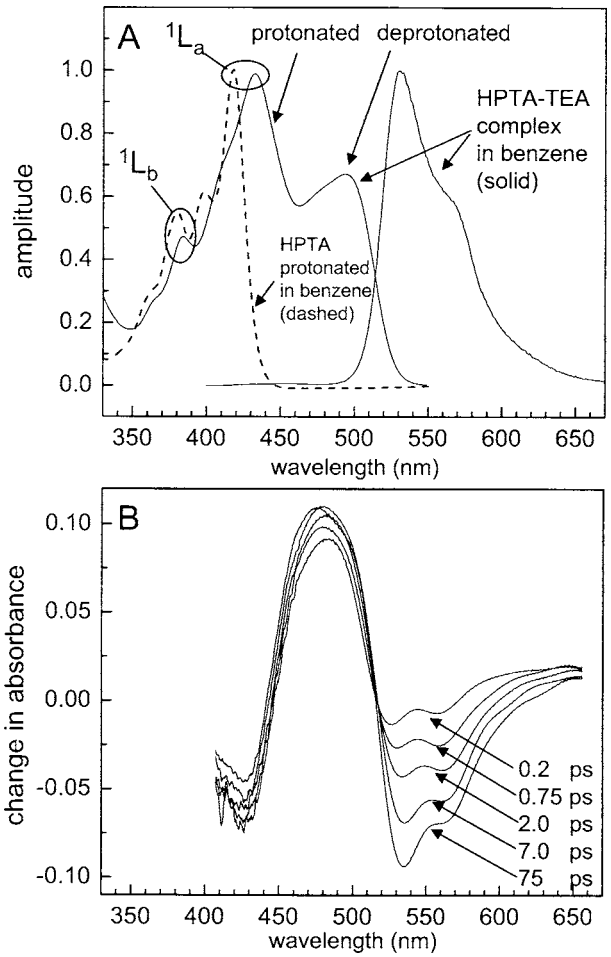

FIG. 9. (A) Absorption and fluorescence spectra of the HPTA-triethylamine complex in benzene (solid). The absorption spectrum of protonated free form of HPTA in benzene is shown for comparison (dashed). (B) The pump-probe spectra of the HPTA-triethylamine complex in benzene at 200 fs, 750 fs, 2 ps, 7 ps, and 75 ps. The 75 ps trace shows the long term limit which is reached in ~20 ps. The feature that grows in has a spectrum that is identical to the fluorescence spectrum shown in (A).

Examining the HPTA-TEA complex it is possible to gain insight into the role that the hydrogen bond coordinate,

$AH\cdots B$, has on the charge redistribution dynamics of HPTA. The absorption and fluorescence spectra of $10^{-4}M$ HPTA in benzene with $10^{-3}M$ TEA are shown in Figure 9(a). As already discussed above, HPTA and TEA form a strong hydrogen bonded complex in the ground state. There is no uncomplexed HPTA in the solution. The presence of the complex can be seen by comparing the absorption spectrum of HPTA with TEA in benzene (solid curve) to the absorption spectrum of HPTA in pure benzene (dashed curve). The absorption spectrum of free HPTA in benzene is blueshifted relative to the HPTA-TEA complex and has a sharper vibronic structure. Evidence of charge redistribution in the ground state caused by the hydrogen bond between HPTA and TEA in the complex can be seen by comparing shifts of the ^1L_a and ^1L_b transitions (see Appendix for assignment of electronic states). The ^1L_a state has more charge transfer character than the ^1L_b state.[19] The ^1L_a transition of the complex is lowered in energy by approximately a factor of 3 (790 cm^{-1}) more than the ^1L_b transition (270 cm^{-1}) because the strong hydrogen bond in the HPTA-TEA complex causes significant charge redistribution.

The hydrogen bond of the HPTA-TEA complex is so strong that even in the electronic ground state, there is substantial presence of the deprotonated form of HPTA, as can be seen in the absorption spectrum shown in Fig. 9(a). The protonated and deprotonated forms are in equilibrium in the ground state. From the absorption coefficients of the protonated and deprotonated states at 400 nm, it was determined that immediately following photoexcitation, 90% of the initial excited-state population is in the protonated state. However, the HPTA-TEA complex fluorescence at 400 nm occurs only from the deprotonated state. The absence of fluorescence from the protonated state demonstrates that the ESPT is very rapid relative to the excited-state lifetime of 1.7 ns.

If the dynamics of hydrogen bonding between the accepting base and the hydroxyl group of the HPTA are responsible for the slow charge redistribution following photoexcitation, as displayed in Figs. 4(a) and 5, then the HPTA-TEA complex should be dramatically different. The HPTA-TEA complex is "primed" for charge redistribution because it already has a strong hydrogen bond configuration between the photoacid hydroxyl group and the accepting amine base prior to photoexcitation. This system should display a very fast charge redistribution, and if the charge redistribution is sufficiently fast, that is, faster than the instrument response (<100 fs), then the only dynamics observed in the spectral evolution will be due to deprotonation. For very fast charge redistribution only two spectral components will be observed in the pump-probe spectrum. These two states will correspond to the intramolecular charge transfer state at the earliest time and evolve into the deprotonated state as time progresses.

The time dependent pump-probe spectra of the HPTA-TEA complex in benzene are displayed in Fig. 9(b). Comparing Figs. 9(b) and 4(a), it is clear that the time dependence of the complexed system is very different from those discussed above. It is apparent that the band that is growing in at 550 nm in Fig. 9(b) is the stimulated emission associated with the HPTA anion formed by proton transfer as it matches the anion fluorescence spectrum in Fig. 9(a). In contrast to Fig. 4(a), the anion stimulated emission band is already evident at 200 fs. There is no evidence of the time dependent spectral changes associated with charge redistribution seen in Fig. 4(a). Therefore, the charge redistribution is faster than the instrument response of ~100 fs. Only two spectral components are visible in the pump-probe spectra and the dynamics can be explained entirely by a one-step process. The first charge redistribution step of the two-step process observed in DMSO is not present for the HPTA-TEA complex. In Fig. 4(a), the pump-probe spectrum starts negative at around 450 nm because of stimulated emission from the protonated state and then turns positive, reflecting excited-state absorption of an intermediate state. This is not observed for the HPTA-TEA complex. Instead, the pump-probe spectrum from 450 to 500 nm starts positive and grows slightly more positive. The change in the pump-probe spectrum occurs almost exclusively in the stimulated emission band with a maximum at 535 nm. As can be seen in Fig. 9(b), most of the dynamics are very rapid, occurring mainly in fewer than 10 ps. The 75 ps curve shows the long term limit of the spectral evolution associated with proton transfer, which is reached in a few tens of picoseconds. The observed dynamics of the HPTA-TEA complex correspond to the second step observed for HPTA in DMSO.

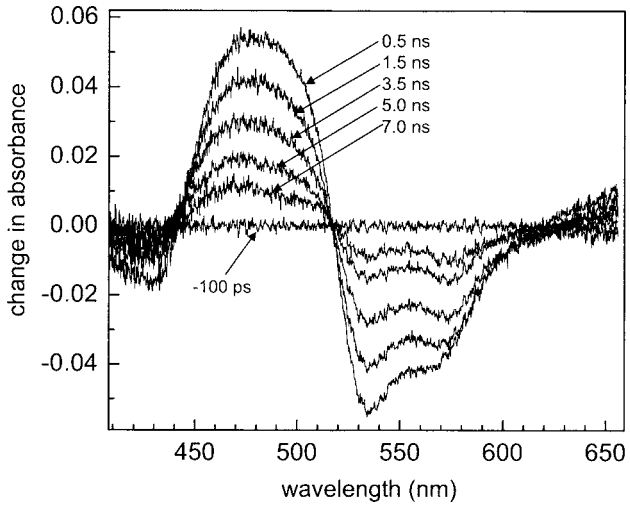

FIG. 10. The long time pump-probe spectra for the HPTA-triethylamine complex in benzene at −100 ps, 0.5 ns, 1.5 ns, 3.5 ns, 5 ns, and 7 ns. The lifetime decay of the deprotonated state immediately returns to the protonated ground state.

The long time scale (nanoseconds) dynamics of the HPTA-TEA complex in benzene are much simpler than those of uncomplexed HPTA in other solvents. Uncomplexed HPTA in other solvents can undergo charge separation of the initially formed contact ion pairs. Because the contact ion pair cannot separate in benzene, upon relaxation of the anion to the ground state, the back reaction proceeds very rapidly to produce the protonated state, which fills in the ground-state bleach in the pump-probe spectrum. Therefore, there is no buildup of the deprotonated state in the electronic ground state. The lack of deprotonated ground state can be seen in Fig. 10 by the uniform decay across all wavelengths. This decay behavior is in contrast to the spectra taken in DMSO

[Fig. 6(b)], which show the appearance of the deprotonated ground state due to solvent separation of ion pairs.

The dynamics of the intramolecular electron transfer reaction are largely controlled by solvent reorganization.[14,18] The experiments on the HPTA-TEA complex suggest that the solvent reorganization that is responsible for charge redistribution in the uncomplexed HPTA solutions is a specific hydrogen bond readjustment between the hydroxyl group of the photoacid and the proton accepting base molecule. Charge redistribution is a necessary step that enables the photoinduced proton transfer process. In many solvents, such as, acetonitrile, glycerol, and benzene, HPTA does not exhibit intramolecular charge transfer and does not undergo excited-state proton transfer.

As shown in DMSO, roughly half of the initial charge transfer step occurs with the solvation time (~2 ps), while the other half of the dynamics occurs on a time scale somewhat greater than 10 ps. It is not clear why roughly half of the charge redistribution process happens on a time scale longer than the general solvation time. However, one explanation is that a specific rearrangement of the solvent is required rather than a more bulk type of restructuring. The specific rearrangement would be the accepting base molecule coming into a particular hydrogen bonding configuration with the hydroxyl of the photoexcited HPTA. Once the proper hydrogen bond geometry is established, the charge redistribution is completed, and proton transfer can occur.

IV. CONCLUDING REMARKS

The results presented here give strong evidence for a relatively slow (tens of picoseconds) intramolecular charge redistribution step in HPTA that precedes the hundreds of picosecond to nanosecond excited-state proton transfer reaction in nonaqueous solvents. The related molecule APTS cannot undergo ESPT. For APTS in strong hydrogen bonding solvents, the time dependent spectroscopic signature reflecting intramolecular charge redistribution is very similar to the first step observed for HPTA in DMSO. When HPTA is complexed with TEA in the ground state, it has a very strong hydrogen bond to the accepting base molecule. In this situation, optical excitation results in very fast charge redistribution. Therefore, it is suggested that formation of a hydrogen bond with the photoacid hydroxyl group is necessary to produce sufficient charge redistribution to permit subsequent proton transfer.

The charge redistribution step, which is evident in Figs. 4 and 5, occurs on two time scales. The first component (~2 ps time scale), which accounts for approximately half of the charge redistribution, is consistent with solvation of the excited state by orientational relaxation of the solvent. However, the second component occurs on an ~13 ps time scale, and only after it is near completion does the anion stimulated emission that arises from proton transfer appears. It is proposed that this slow step is the formation of an appropriate geometry hydrogen bond between the HPTA hydroxyl group and a solvent molecule, which is the base in the proton transfer reaction.

From the results presented here, it is clear that the charge redistribution process responsible for photoacidity does not necessarily occur directly upon optical excitation. The time scale for charge redistribution may be significantly longer than the general solvation time. The formation of the charge transfer state is a distinct step, which can be seen on time scales as long as tens of picoseconds.

The charge redistribution prior to proton transfer observed for HPTA has implications for the dynamics of other photoacids with strong electron withdrawing groups that facilitate intramolecular charge redistribution. For example, HPTS displays biexponential excited-state proton transfer dynamics.[24] HPTS shows a relatively fast (~3 ps) decay and a slower (~90 ps) decay in water.[11,12,24] The ~90 ps component is due to ESPT, but the cause of the 3 ps dynamics is less clear. The spectral responses for the two components are not as easily separated for HPTS as they are for HPTA. There have been arguments that both the 3 and 90 ps components are caused by ESPT,[11,12] but also that the 3 ps component arises from an intramolecular charge redistribution process.[25–27] Solvation dynamics of similar dye molecules in water happen on a time scale slightly under 1 ps, and a Stokes shift with this time is observed for HPTS,[12] which makes it difficult to attribute the 3 ps decay to a simple solvation process. For HPTA in DMSO, a large part of the intramolecular charge redistribution step occurs on a time scale significantly longer than the general solvation time. We will show in a subsequent publication by examination of a variety of pyrene photoacids that the dynamics of HPTS and HPTA have the same mechanism; that is, the first step (following the Stokes shift) is intramolecular charge redistribution followed by ESPT on a longer time scale.

ACKNOWLEDGMENTS

This work was supported by the Department of Energy (No. DE-FG03-84ER13251). D. B. Spry thanks the National Science Foundation for a NSF Fellowship.

APPENDIX: SPECTROSCOPIC STATES

In characterizing the electronic states of HPTA, it is useful to make a comparison to its better known relative, HPTS. The electron withdrawing substituents of HPTA are stronger than the sulfonate groups of HPTS. This can be seen by comparing the inductive Hammett substituent constants (σ_I) of the two functional groups (0.28 and 0.44 for–SO_3^- and–$SO_2N(CH_3)_2$, respectively).[28] The increased electron withdrawing strength of the substituents of HPTA more effectively couples the electron density of the hydroxyl group to the π system of the pyrene moiety.

The absorption spectra of the protonated forms of HPTA and HPTS are shown in Fig. 11(a), and the corresponding spectra for the deprotonated forms are shown in Fig. 11(b). The electronic states of both the protonated and deprotonated forms of HPTS have been previously identified with fluorescence polarization anisotropy and magnetic circular dichroism spectroscopies.[19] In referring to the electronic states here, we will use the notation of Pratt.[29] It is well-known that the ^1L_a state of most aromatic molecules, including pyrene,[30] is preferentially lowered in energy over the ^1L_b state upon

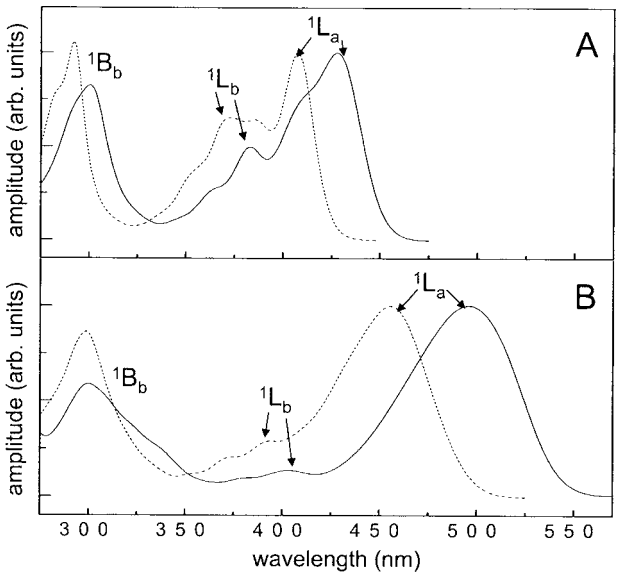

FIG. 11. (A) The absorption spectra for the protonated forms of HPTA (solid) and HPTS (dotted). (B) The absorption spectra of the deprotonated forms of HPTA (solid) and HPTS (dotted). All spectra were taken in glycerol at room temperature.

the addition of a π-donating substituent.[31,32] Increasing the strength of the inductive electron withdrawing groups to pull electron density from the hydroxyl group to the ring is analogous to increasing the π-donating ability of the hydroxyl group. The increased strength of the withdrawing groups redshifts the position of the ^1L_a band to a larger extent than the ^1L_b band in HPTA and further separates the two transitions relative to HPTS, which can be seen in Figs. 11(a) and 11(b). By comparing the transition peaks of HPTA to HPTS in the protonated state, the ^1L_a transition of HPTA shifts to a lower energy by 1200 cm^{-1} and the ^1L_b transition shifts by 700 cm^{-1}. The difference between the two transitions is more dramatic in the deprotonated state. In the deprotonated state the ^1L_a band of HPTA shifts to a lower energy by 1800 cm^{-1} and the ^1L_b band shifts by 600 cm^{-1}.

[1] T. Elsaesser and H. J. Bakker, *Ultrafast Hydrogen Bonding Dynamics and Proton Transfer Processes in the Condensed Phase* (Kluwer, Dordrecht, 2002).
[2] Z. Rappoport, *The Chemistry of Phenols* (Wiley, New York, 2003).
[3] R. P. Bell, *The Proton in Chemistry*, 2nd ed. (Chapman and Hall, London, 1973).
[4] E. F. Caldin and V. Gold, *Proton-Transfer Reactions* (Chapman and Hall, London, 1975).
[5] A. Weller, Z. Phys. Chem. (Leipzig) **17**, 224 (1958).
[6] T. Förster, Z. Elektrochem. **54**, 531 (1950).
[7] J. F. Ireland and P. A. H. Wyatt, Adv. Phys. Org. Chem. **12**, 131 (1976).
[8] A. Weller, Prog. React. Kinet. **1**, 187 (1961).
[9] M. Eigen, W. Kruse, G. Maass, and L. De Maeyer, Prog. React. Kinet. **2**, 285 (1964).
[10] N. Agmon, J. Phys. Chem. A **109**, 13 (2005).
[11] P. Leiderman, L. Genosar, and D. Huppert, J. Phys. Chem. A **109**, 5965 (2005).
[12] D. B. Spry, A. Goun, and M. D. Fayer, J. Phys. Chem. A **111**, 230 (2007).
[13] M. L. Horng, J. A. Gardecki, A. Papazyan, and M. Maroncelli, J. Phys. Chem. **99**, 17311 (1995).
[14] E. M. Kosower and D. Huppert, Annu. Rev. Phys. Chem. **37**, 127 (1986).
[15] D. Huppert, S. D. Rand, P. M. Rentzepis, P. F. Barbara, W. S. Sturve, and Z. R. Grabowski, J. Chem. Phys. **75**, 5714 (1981).
[16] *Ultrafast Processes in Chemistry and Photobiology*, edited by M. A. El-Sayed, I. Tanaka, and Y. Molin (Blackwell Science, Oxford, 1995).
[17] G. C. Walker, E. Akesson, A. E. Johnson, N. E. Levinger, and P. F. Barbara, J. Phys. Chem. **96**, 3728 (1992).
[18] E. M. Kosower and D. Huppert, Chem. Phys. Lett. **96**, 433 (1983).
[19] D. B. Spry, A. Goun, and M. D. Fayer, J. Chem. Phys. **125**, 144514 (2006).
[20] W. Jarzeba, G. C. Walker, A. E. Johnson, and P. F. Barbara, J. Chem. Phys. **152**, 57 (1991).
[21] K. M. Solntsev, D. Huppert, and N. Agmon, J. Phys. Chem. A **103**, 6984 (1999).
[22] K. M. Solntsev, D. Huppert, L. M. Tolbert, and N. Agmon, J. Am. Chem. Soc. **120**, 7981 (1998).
[23] E. Pines, D. Pines, Y.-Z. Ma, and G. R. Fleming, ChemPhysChem **5**, 1315 (2004).
[24] C. Prayer, T. Gustavsson, and T. H. Tran-Thi, Proceedings of the 54th International Meeting of Physical Chemistry, France, 1996 (unpublished).
[25] O. F. Mohammed, J. Dreyer, B.-Z. Magnes, E. Pines, and E. T. J. Nibbering, ChemPhysChem **6**, 625 (2005).
[26] J. T. Hynes, T.-H. Tran-Thi, and G. Granucci, J. Photochem. Photobiol., A **154**, 3 (2002).
[27] T. H. Tran-Thi, C. Prayer, P. Millie, P. Uznanski, and J. T. Hynes, J. Phys. Chem. A **106**, 2244 (2002).
[28] C. Hansch, A. Leo, and R. W. Taft, Chem. Rev. (Washington, D.C.) **91**, 165 (1991).
[29] J. R. Platt, J. Chem. Phys. **17**, 484 (1949).
[30] V. Baliah and M. K. Pillay, Indian J. Chem. **9**, 815 (1971).
[31] J. N. Murrell, *The Theory of the Electronic Spectra of Organic Molecules* (Wiley, New York, 1964).
[32] M. Klessinger and J. Michl, *Excited States and Photochemistry of Organic Molecules* (VCH, New York, 1994).